

# Vibrational Levels of Ar<sub>4</sub>: New Odd-Parity Bosonic States<sup>†</sup>

Xiao-Gang Wang\* and Tucker Carrington, Jr.\*

Département de chimie, Université de Montréal, C.P. 6128, succursale Centre-ville,  
Montréal (Québec) H3C 3J7, Canada

Received: February 2, 2007; In Final Form: March 5, 2007

Vibrational levels of Ar<sub>4</sub> are computed using the Lanczos algorithm and a large basis set. We find both even- and odd-parity states with wave functions that are invariant with respect to permutations of the Ar atoms. The odd-parity bosonic levels have not been computed previously. The even-parity levels are close to those obtained using the correlation-function Monte Carlo method (CFMC).

## I. Introduction

The only reliable, systematically improvable methods for computing energy levels of molecules and clusters rely on basis functions. For many molecules, low-lying levels can be obtained using approaches based on perturbation theory, but for loosely bound clusters, even the lowest levels must be determined by computing eigenvalues of a Hamiltonian matrix representing the Hamiltonian operator in a basis.<sup>1–3</sup> The cost of such a calculation scales poorly with basis set size. The simplest basis functions are products of functions of a single variable. If a full direct product basis is used, many product functions are required to calculate even the lowest energy levels.<sup>4</sup> Omitting some of the product functions enables one to drastically reduce the number of basis functions.<sup>5–11</sup> Direct product and nondirect product contracted functions<sup>12–21</sup> allow one to compute accurate spectra of molecules (or clusters) with several atoms.<sup>11,22–26</sup> It is nevertheless clear that, even using contracted basis functions, calculations for clusters with many atoms are not possible.

The correlation-function Monte Carlo method (CFMC)<sup>27,28</sup> appears to be very promising. It does use basis functions, but a Monte Carlo imaginary-time projection method is used to obtain a very compact basis. The Monte Carlo imaginary-time projector removes wave functions with larger energies from a starting basis of optimized many-parameter trial functions. Overlap and Hamiltonian matrix elements are computed in the final Monte Carlo projected basis, and a small generalized eigenvalue problem is solved. This method has been used to compute bound-state energies for several molecules.<sup>28–31</sup> In an impressive paper, Nightingale and Melik-Alaverdian<sup>30</sup> computed vibrationally excited levels of Ar<sub>*n*</sub> with *n* up to 7 using the CFMC method and forcing trial functions to be invariant with respect to permutation of Ar atoms. More accurate Ar<sub>4</sub> levels were later published in ref 32. Given the floppy nature of Ar clusters, Ar<sub>7</sub> is certainly well beyond the reach of standard contracted basis set methods. For Ar<sub>3</sub> and other rare-gas trimers, CFMC results have been compared with levels computed with direct product basis sets.<sup>31,33</sup>

The goal of this paper is twofold. First, for Ar<sub>4</sub>, we compare energy levels computed with a product basis Lanczos method to those obtained by Nightingale and Melik-Alaverdian. Second, we present, for the first time, Ar<sub>4</sub> energy levels whose wave

functions have odd parity. Because Ar is a boson, we denote these odd-parity bosonic states. Nightingale and Melik-Alaverdian did not calculate the odd-parity states because the trial basis functions (and hence the MC projected functions) they used depend only on the interatomic distances of Ar<sub>4</sub>. The interatomic distances are all invariant under the inversion operation, and therefore, basis functions that depend only on the interatomic distances are invariant under the inversion operation; none of their basis functions have odd parity.<sup>34</sup> Using the same type of trial basis functions to compute levels of Ar<sub>3</sub>, one does not miss levels.<sup>33</sup> This is due to the fact that molecules or clusters with fewer than four atoms have no odd-parity vibrational levels. Four-atom clusters have odd-parity levels because at least one of the coordinates used to specify the shape of the cluster is effected by the inversion operator. Blume and Greene have also computed even-parity levels of Ar<sub>4</sub>.<sup>35</sup> They use an adiabatic hyperspherical approach. They missed the odd-parity levels because they computed only the lowest bend level for each hyperspherical radius value.

Our basis set calculation yields both levels whose wave functions are invariant under permutation of any two atoms and levels that are missing in nature because their wave functions are not invariant under permutation of any two atoms. We must be able to distinguish between the two groups. If our levels were labeled by irreducible representations of the full symmetry group of Ar<sub>4</sub>, this would be easy. We use (Jacobi) coordinates in which the kinetic energy operator (KEO) is simple but that do not allow us to exploit all of the symmetry of Ar<sub>4</sub>. Instead, we exploit some of the symmetry and work in a subgroup of the full symmetry group and obtain levels labeled by irreducible representations of the subgroup. We call the subgroup the coordinate symmetry group. We use the correlation between the full symmetry group and the coordinate symmetry group to assign, without examining the wave functions, irreducible representations of the full symmetry group to the computed levels.

## II. Hamiltonian and Basis Functions

The coordinates we use are the spherical polar coordinates associated with the diatom–diatom Jacobi vectors (see the upper panel of Figure 1). The KEO is well-known.<sup>36</sup> The notation we use is the same as that of ref 37. The potential is a sum of Lennard-Jones potentials, one for each pair of atoms. It is the same as the potential used in ref 30 and is written in terms of scaled coordinates. The scaled Lennard-Jones potential is

<sup>†</sup> Part of the special issue “Robert E. Wyatt Festschrift”.

\* E-mail: Xiaogang.Wang@umontreal.ca; Tucker.Carrington@umontreal.ca.

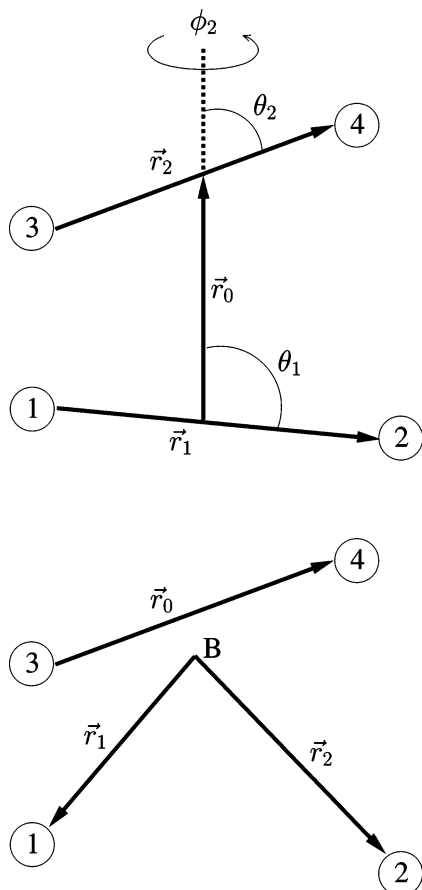


**Figure 1.** Diatom–diatom Jacobi (upper) and satellite (lower) vectors. Definitions of the angles for the satellite vectors are the same as those of the Jacobi vectors and are not shown. For the satellite vectors, *B* is the position of the canonical point on the line joining the center of mass of atoms 3 and 4 and center of mass of atoms 1 and 2 and depends on the masses and positions of the nuclei.

$r^{-12} - 2r^{-6}$ , where  $r$  is a scaled interatomic distance. In the KEO of ref 37, the mass of each of the atoms is replaced by the dimensionless mass  $\mu = 2^{1/3}m\sigma^2\epsilon$ , where  $m$  is the mass of the Ar nucleus, and  $\sigma$  and  $\epsilon$  are the core radius and well depth of the unscaled Lennard-Jones potential, respectively. We use the same value as Nightingale and Melik-Alaverdian,  $\mu^{-1} = 6.9635 \times 10^{-4}$ .<sup>30</sup>

The basis functions we use are products of parity-adapted bend and stretch functions. The parity-adapted bend functions we use are

$$|u_{l_1 l_2 m_2}^p\rangle = N_{m_2} \frac{1}{\sqrt{2}} [|l_1 l_2 m_2\rangle + (-1)^p |l_1 l_2 \bar{m}_2\rangle] \quad (1)$$

with  $N_{m_2} = (1 + \delta_{m_2,0})^{-1/2}$ , where  $P = 0$  and  $1$  correspond to even and odd parity, respectively, and  $m_2 \geq 0$ . If  $P = 1$ ,  $m_2 = 0$  is not allowed. These basis functions are linear combinations of

$$\langle \theta_1, \theta_2, \phi_2 | l_1 l_2 m_2 \rangle = \sqrt{\frac{1}{2\pi}} \Theta_{l_1}^{m_1}(\theta_1) \Theta_{l_2}^{m_2}(\theta_2) e^{im_2\phi_2} \quad (2)$$

where  $\Theta_l^m(\theta)$  is a normalized associated Legendre function with the  $(-1)^m$  Condon–Shortley phase factor<sup>38</sup> and  $m_1 \equiv -m_2$ . Note that the inversion operator  $E^*$  affects a function of the vibrational coordinates<sup>39</sup>

$$E^* f(r_0, r_1, r_2, \theta_1, \theta_2, \phi_2) = f(r_0, r_1, r_2, \theta_1, \theta_2, -\phi_2) \quad (3)$$

However, it does not affect a function of the vibrational coordinates of molecules with fewer than four atoms because such molecules have no dihedral coordinates. It is for this reason that odd-parity vibrational states only exist for molecules with more than three atoms. The stretch functions are products of three potential-optimized discrete-variable representation<sup>40,41</sup> (PODVR) functions, and the 6-d basis functions are therefore

$$g_{\alpha_0}(r_0)g_{\alpha_1}(r_1)g_{\alpha_2}(r_2)u_{l_1 l_2 m_2}^p(\theta_1, \theta_2, \phi_2) \quad (4)$$

where the  $g_{\alpha_i}(r_i)$  are the PODVR functions. The PODVRs for  $r_1$  and  $r_2$  are identical and computed from a reference potential obtained by setting all other coordinates to their equilibrium values. The PODVR for  $r_0$  is discussed in the next section.

### III. Choosing $r_0$ Basis Functions to Account for Conversion Between Two Equilibrium Structures

The dimensionless pairwise additive Ar<sub>4</sub> potential has two equivalent tetrahedral equilibrium structures with  $V = -6.0$ . The two rearrangement pathways are illustrated in Figure 2. We call them insertion and torsion. They share one saddle point at  $V = -5.07$ , where Ar<sub>4</sub> is a rhombus (diamond-like equilateral quadrangle). Proceeding along the insertion pathway,  $r_0$  decreases until one of the Ar–Ar diatomics is inserted into the other Ar–Ar diatomic. The rhombus saddle point is at  $r_0 = 0$ . Proceeding along the torsion pathway, one Ar–Ar diatomic rotates about the interdiatomic axis,  $\theta_2$  changes from 90 to 60 (at the saddle point) to 90°, and  $\phi_2$  changes from 90 to 0 (at the saddle point) to -90°.

The calculations are done with a KEO written for use with a volume element  $dr_0 dr_1 dr_2 \sin(\theta_1) d\theta_1 \sin(\theta_2) d\theta_2 d\phi_2$ . The true wave function is related to  $\Psi$ , the wave function we compute, by  $\Psi_{\text{true}} = (r_0 r_1 r_2)^{-1} \Psi$ . The KEO is singular if  $r_0 = 0$  or  $r_1 = 0$  or  $r_2 = 0$ . Only the  $r_0 = 0$  singularity is important because, if  $r_1 = 0$  or  $r_2 = 0$ , the wave functions are all very small. To ensure that all KEO matrix elements are finite, one must choose basis functions that behave as  $r_0^p$  (with  $p \geq 1$ ) close to  $r_0 = 0$ . Such basis functions remove the singularity in the integral of the KEO terms with  $1/r_0^2$ . A good way to cope with the singularity is to use spherical oscillator basis functions.<sup>42,43</sup> Spherical oscillator basis functions matrix elements are finite, and spherical oscillator basis functions have the additional advantage that, if the order of the Laguerre polynomials is chosen correctly,<sup>43</sup> they behave correctly near  $r_0 = 0$ . Instead of spherical oscillator functions, we have used a PODVR built from sine functions. Because sine functions approach 0 linearly as  $r_0$  approaches 0, the sine-basis matrix elements are all finite. They are not exact eigenfunctions of a piece of the KEO, but they do include potential information and are easier to use. To define the PODVR for  $r_0$ , we use a reference potential defined by setting bend coordinates equal to equilibrium values and minimizing the potential with respect to  $r_1$  and  $r_2$ . The resulting potential is flat close to  $r_0 = 0$ . The 24 PODVR functions defined in the range [0.0, 4.0] are used.

### IV. Symmetry Assignment Using Correlation Between the Molecular Symmetry Group and the Coordinate Symmetry Groups

As mentioned briefly in the Introduction, it is frequently the case that one wishes to use coordinates with which it is not possible to exploit the full symmetry. The full symmetry cannot be exploited if one of the operations in the molecular symmetry group, when applied to one of the basis functions, yields a function that is not a linear combination of basis functions. In

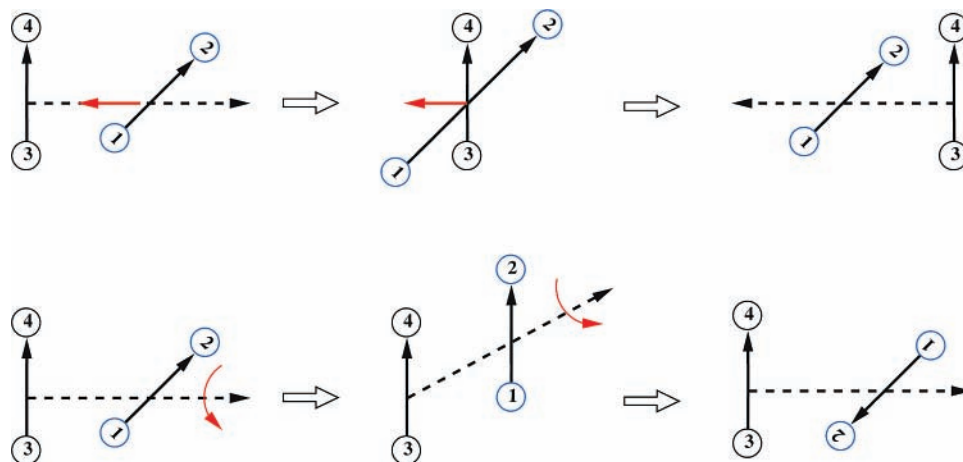


**Figure 2.** Two rearrangement pathways between two equilibrium structures, insertion (upper) and torsion (lower).

**TABLE 1: Character Table of  $S_4$ , Taken from Table 5-3 of Ref 44**

Sym	E	(12)	(12) (34)	(123)	(1234)
	1	6	3	8	6
<i>A</i>	1	1	1	1	1
<i>B</i>	1	-1	1	1	-1
<i>E</i>	2	0	2	-1	0
<i>F</i>	3	1	-1	0	-1
<i>G</i>	3	-1	-1	0	1

this paper, we call the group composed of operators, which when applied to any of the basis functions gives a function in the basis, the coordinate symmetry group. The coordinate symmetry group is a subgroup of the molecular symmetry group.

The molecular symmetry group of  $\text{Ar}_4$  is the permutation-inversion group  $G_{48} = \{E, E^*\} \otimes S_4$ , where  $\{E, E^*\}$  is the inversion group and  $S_4$  is the permutation group of four identical particles.<sup>44</sup> The coordinate symmetry group is  $G_{16} = \{E, E^*\} \otimes G_8$ , where  $G_8 = \{E, (12)\} \otimes \{E, (34)\} \otimes \{E, (13)(24)\}$  is a permutation group. Operators not in the coordinate symmetry group are excluded because, when we operate with them on basis functions, we do not obtain functions in the basis. For example, (13) is excluded because the new coordinates obtained by operating with (13) are complicated functions of the old coordinates, and therefore, acting with (13) on a basis function of the old coordinates gives a complicated function which is not in the basis.

One is therefore forced to work in the coordinate symmetry group and can easily obtain levels labeled by the irreducible representations of the coordinate symmetry group but would like to label the levels with irreducible representations of the molecular symmetry group. For  $\text{Ar}_4$ , we can do this by using the correlation table between  $S_4$  and  $G_8$ . To make the correlation table, we need character tables for  $S_4$  and  $G_8$ . The character table of the  $S_4$  group is given in ref 44 and reproduced in Table 1. We take the character table for  $G_8$  from ref 45 where it was used to study  $(\text{H}_2\text{O})_2$ . It is reproduced in Table 2, but the symmetry labels of Dyke are renamed. We label states that are symmetric/antisymmetric with respect to (13)(24) with *A/B*, whereas Dyke used *A/B* for symmetry with respect to (1324). Following Dyke, we label states that are symmetric with respect to either (12) or (34) with 1/2. From the character tables of  $G_8$  and  $S_4$ , the corresponding correlation table is derived and presented in Table 3. Using the correlation table and the computed energy levels, we can establish a mapping between irreducible representations of  $G_8$  and those of  $S_4$  (and hence between irreducible representations of  $G_{16}$  and those of  $G_{24}$ ). *A*<sub>1</sub> and *A*<sub>2</sub> levels that are very close (and become degenerate as

**TABLE 2: Character Table of  $G_8^a$**

This Work	Dyke <sup>45</sup>	E	(12) (34)	(13) (24) (14) (23)	(12) (34)	(1324) (1423)
<i>A</i> <sub>1</sub>	<i>A</i> <sub>1</sub>	1	1	1	1	1
<i>B</i> <sub>1</sub>	<i>B</i> <sub>1</sub>	1	1	-1	1	-1
<i>A</i> <sub>2</sub>	<i>B</i> <sub>2</sub>	1	-1	1	1	-1
<i>B</i> <sub>2</sub>	<i>A</i> <sub>2</sub>	1	-1	-1	1	1
<i>E</i>	<i>E</i>	2	0	0	-2	0

<sup>a</sup> The  $G_{16}$  symmetry labels are obtained by adding a  $\pm$  superscript (corresponding to even/odd parity, respectively) to the corresponding  $G_8$  symmetry labels.

**TABLE 3: Correlation Table between  $S_4$  and  $G_8$**

$S_4$	$G_8$
<i>A</i>	<i>A</i> <sub>1</sub>
<i>B</i>	<i>A</i> <sub>2</sub>
<i>E</i>	<i>A</i> <sub>1</sub> + <i>A</i> <sub>2</sub>
<i>F</i>	<i>B</i> <sub>1</sub> + <i>E</i>
<i>G</i>	<i>B</i> <sub>2</sub> + <i>E</i>

the basis size is increased) are *E* levels in  $S_4$ . *B*<sub>1</sub> and *E* levels that are very close are *F* levels in  $S_4$ . *B*<sub>2</sub> and *E* levels that are very close are *G* levels in  $S_4$ . *A*<sub>1</sub> levels that are not very close to other levels are *A* levels in  $S_4$ , and *A*<sub>2</sub> levels that are not very close to other levels are *B* levels in  $S_4$ . Splittings between levels which become degenerate as the basis size is increased are lower bounds of the error in the finite basis results. We previously used this correlation table technique to assign symmetry labels of bend states of  $\text{CH}_4$ .<sup>46</sup>

## V. Computational Details

In Table 4, we summarize the action of symmetry operations on coordinates and basis functions for four-atom molecules. The effect of (12), (34), and (13)(24) on our basis functions is given in the diatom–diatom section of the table. Combining these results with the factorization  $G_8 = \{E, (12)\} \otimes \{E, (34)\} \otimes \{E, (13)(24)\}$ , we deduce that basis functions with  $l_1$  even and  $l_2$  even transform like *A*<sub>1</sub> or *B*<sub>1</sub>; basis functions with  $l_1$  odd and  $l_2$  odd transform like *A*<sub>2</sub> or *B*<sub>2</sub>; basis functions with  $l_1$  ( $l_2$ ) even and  $l_2$  ( $l_1$ ) odd transform like *E*. We can, therefore, do separate calculations for the three cases: (i)  $l_1 = \text{even}$ ,  $l_2 = \text{even}$ ; (ii)  $l_1 = \text{odd}$ ,  $l_2 = \text{odd}$ ; and (iii)  $l_1 = \text{even}$ ,  $l_2 = \text{odd}$ . For case (i), we make a projection operator for (13)(24) and use the symmetry-adapted Lanczos (SAL) method<sup>47,48</sup> to determine *A*<sub>1</sub> and *B*<sub>1</sub> levels. Similarly for case (ii), we determine *A*<sub>2</sub> and *B*<sub>2</sub> levels.

For the bend basis functions, we use  $l_{\text{max}} = m_{\text{max}} = 38, 41$  Gauss–Legendre quadrature points for  $\theta_1$  and  $\theta_2$ , and 81 equally

**TABLE 4: Symmetry Operations for a System of Four Identical Atoms;  $\bar{m} = -m$** 

operations	effect on $f(\theta_1, \theta_2, \phi_2; \alpha, \beta, \gamma)$	effect on $ l_1 l_2 m_2; JKM\rangle$	effect on $u_{l_1 l_2 m_2; K}^{JMP}$	effect on vectors
Diatom–Diatom Jacobi Vectors (Figure 1a)				
(12)	$f(\pi - \theta_1, \theta_2, \phi_2 + \pi; \alpha, \beta, \gamma + \pi)$	$(-1)^{l_1}  l_1 l_2 m_2; JKM\rangle$	$(-1)^{l_1} u_{l_1 l_2 m_2; K}^{JMP}$	flip of $\mathbf{r}_1$
(34)	$f(\theta_1, \pi - \theta_2, \phi_2 + \pi; \alpha, \beta, \gamma)$	$(-1)^{l_1}  l_1 l_2 m_2; JKM\rangle$	$(-1)^{l_2} u_{l_1 l_2 m_2; K}^{JMP}$	flip of $\mathbf{r}_2$
(13)(24)	$f(\pi - \theta_2, \pi - \theta_1, \phi_2; \pi + \alpha, \pi - \beta, -\gamma - \phi_2)$	$(-1)^{J+l_1+l_2}  l_2 l_1 \bar{m}_1; \bar{J}\bar{K}\bar{M}\rangle$	$(-1)^{l_1+l_2+P} u_{l_2 l_1 \bar{m}_1; \bar{K}}^{JMP} (K > 0)$ $(-1)^{l_1+l_2+J} u_{l_2 l_1 \bar{m}_1; 0}^{JMP} (K = 0)$	flip of $\mathbf{r}_0$ , exchange of $\mathbf{r}_1$ and $\mathbf{r}_2$
Satellite Vectors (Figure 1b)				
(12)	$f(\theta_2, \theta_1, -\phi_2; \alpha, \beta, \gamma + \phi_2)$	$ l_2 l_1 m_1; JKM\rangle$	$u_{l_2 l_1 m_1; K}^{JMP} (K > 0)$ $(-1)^{J+P} u_{l_2 l_1 \bar{m}_1; 0}^{JMP} (K = 0)$	exchange of $\mathbf{r}_1$ and $\mathbf{r}_2$
(34)	$f(\pi - \theta_1, \pi - \theta_2, -\phi_2; \pi + \alpha, \pi - \beta, -\gamma)$	$(-1)^{J+l_1+l_2}  l_1 l_2 \bar{m}_2; \bar{J}\bar{K}\bar{M}\rangle$	$(-1)^{l_1+l_2+P} u_{l_1 l_2 \bar{m}_2; K}^{JMP}$	flip of $\mathbf{r}_0$
Any Vectors				
$E^*$	$f(\theta_1, \theta_2, -\phi_2; \pi + \alpha, \pi - \beta, \pi - \gamma)$	$(-1)^J  l_1 l_2 \bar{m}_2; \bar{J}\bar{K}\bar{M}\rangle$	$(-1)^P u_{l_1 l_2 m_2; K}^{JMP}$	flip of $\mathbf{r}_0, \mathbf{r}_1, \mathbf{r}_2$

**TABLE 5: Vibrational Levels of Ar<sub>4</sub> (up to  $-4.40$ )<sup>a</sup>**

$A_1^+ (A_2^-)$	$B_1^+ (B_2^-)$	$A_2^+ (A_1^-)$	$B_2^+ (B_1^-)$	$E^+ (E^-)$
<b>-5.1181</b> $A^+ (B^-)$	-4.8610 $F^+ (G^-)$	-4.9327 $E^+ (E^-)$	-4.6710 $G^+ (F^-)$	-4.8610 $F^+ (G^-)$
-4.9327 $E^+ (E^-)$	-4.7080 $F^+ (G^-)$	-4.7520 $E^+ (E^-)$	-4.5166 $G^+ (F^-)$	-4.7080 $F^+ (G^-)$
<b>-4.8008</b> $A^+ (B^-)$	-4.6049 $F^+ (G^-)$	-4.6617 $E^+ (E^-)$	-4.4600 $G^+ (F^-)$	-4.6709 $G^+ (F^-)$
-4.7521 $E^+ (E^-)$	-4.5846 $F^+ (G^-)$	-4.6172 $E^+ (E^-)$	-4.4180 $G^+ (F^-)$	-4.6051 $F^+ (G^-)$
<b>-4.7250</b> $A^+ (B^-)$	-4.5359 $F^+ (G^-)$	<b>-4.5682</b> $B^+ (A^-)$		-4.5847 $F^+ (G^-)$
-4.6617 $E^+ (E^-)$	-4.4841 $F^+ (G^-)$	-4.5569 $E^+ (E^-)$		-4.5358 $F^+ (G^-)$
<b>-4.6299</b> $A^+ (B^-)$	-4.4774 $F^+ (G^-)$	-4.5216 $E^+ (E^-)$		-4.5165 $G^+ (F^-)$
-4.6172 $E^+ (E^-)$	-4.4332 $F^+ (G^-)$	-4.4756 $E^+ (E^-)$		-4.4840 $F^+ (G^-)$
<b>-4.5861</b> $A^+ (B^-)$	-4.4287 $F^+ (G^-)$	-4.4622 $E^+ (E^-)$		-4.4772 $F^+ (G^-)$
-4.5570 $E^+ (E^-)$	-4.4029 $F^+ (G^-)$	<b>-4.4380</b> $B^+ (A^-)$		-4.4603 $G^+ (F^-)$
<b>-4.5278</b> $A^+ (B^-)$		-4.4292 $E^+ (E^-)$		-4.4336 $F^+ (G^-)$
-4.5215 $E^+ (E^-)$		-4.4016 $E^+ (E^-)$		-4.4287 $F^+ (G^-)$
<b>-4.4834</b> $A^+ (B^-)$				-4.4180 $G^+ (F^-)$
-4.4756 $E^+ (E^-)$				-4.4045 $F^+ (G^-)$
<b>-4.4631</b> $A^+ (B^-)$				
-4.4623 $E^+ (E^-)$				
-4.4291 $E^+ (E^-)$				
<b>-4.4279</b> $A^+ (B^-)$				
-4.4013 $E^+ (E^-)$				

<sup>a</sup> The columns are labeled by irreducible representations of the coordinate symmetry group. Symmetry labels after each level are for the molecular symmetry group. Each level has two molecular symmetry group labels because even- and odd-parity levels are equal to the number of digits given. Bosonic levels ( $A^+$  or  $A^-$ ) are in bold.

spaced, equal weight points in the range  $[0, 2\pi]$  for  $\phi_2$ . For  $r_1$  and  $r_2$ , we use 10 PODVR<sup>40,41</sup> functions obtained from eigenfunctions of a 1D cut potential in the range  $[0.5, 5.0]$ . Note that the potential cut we use does not correspond to Ar<sub>4</sub> dissociating to Ar + Ar<sub>3</sub>, and at large  $r_i$ , our reference potential is steeper than the reference potential that dissociates to Ar + Ar<sub>3</sub>. Nonetheless, the long-range behavior of our reference potential is not biasing our results because its range is large enough. As explained in Section III, we choose  $r_0 = 0$  basis functions to ensure that the true wave function at  $r_0 = 0$  is finite and possibly nonzero. The reference potential for the PODVR we use is defined there. The direct product basis function size is 12.8, 11.9, and 12.3 million for the  $A_1^+ + B_1^+, A_2^+ + B_2^+$ , and  $E^+$  symmetry blocks, respectively, and 11.0, 11.9, and 11.4 million for  $A_2^- + B_2^-, A_1^- + B_1^-$ , and  $E^-$  symmetry blocks, respectively. A potential ceiling is imposed to reduce the spectral range and, hence, accelerate convergence of the Lanczos calculation.<sup>43</sup> We found that a ceiling value of 500 introduces errors smaller than  $10^{-4}$ .

We use the diagonal approximation for the PODVR matrix elements of  $r_0^{-2}$  in the KEO. This approximation is poor when

**TABLE 6: A Comparison of Bosonic Levels of This Work and Those Computed with the CFMC Method<sup>32,a</sup>**

parity	ref 32	this work
+	-5.11814605	-5.1181
+	-4.80089773	-4.8008
+	-4.7251567	-4.7250
+	-4.630025	-4.6299
+	-4.586389	-4.5861
-		-4.5682
+		-4.5278
+		-4.4834
+		-4.4631
-		-4.4380
+		-4.4279

<sup>a</sup> The +/- refer to even/odd parity.

$r_0$  is small,<sup>49</sup> but we find that levels computed with and without the approximation are the same to 5 significant digits. To avoid the approximation, we compute numerically exact matrix elements in the primitive sine basis (using a Simpson's rule with enough points) and transform to the 1-d eigenfunction basis and then to the PODVR basis. For higher energy levels for

which the amplitude of the wave function is larger close to  $r_0 = 0$ , avoiding the approximation would be more important. The diagonal approximation has the advantage that the matrix–vector products are faster.

## VI. Results

All of the vibrational levels up to  $-4.40$  are given in Table 5. Convergence errors are estimated to be smaller than 0.0005 by comparing with levels obtained with larger basis sets. Each column is labeled with an irreducible representation of the coordinate symmetry group  $G_{16}$ . Even- and odd-parity levels are split by less than 0.0001, indicating a slow rearrangement between the two equilibrium versions. According to a previous variational Monte Carlo study using a very similar potential, the ground state has no amplitude in the saddle region.<sup>50</sup> As discussed in Section IV, using the correlation table, we determine the symmetry labels of the molecular symmetry group that appear with each level in Table 5. Levels in different columns that are degenerate must be  $E$ ,  $F$ , or  $G$  in  $S_4$ , and the remaining levels must be  $A$  or  $B$ . Only the  $A^+$  and  $A^-$  states are permutation invariant. Note that the lowest  $A^-$  state has higher energy than five  $A^+$  states. We can compare the even-parity levels with those obtained by Nightingale et al. using the CFMC method. The ground-state energy we compute agrees well with the result ( $-5.11881$ ) of ref 30. For excited states, the new numbers reported in ref 32 agree with our results; see Table 6. The energy levels<sup>35</sup> obtained using the adiabatic hyperspherical approach have larger errors because it is an approximate method.

The fact that the splittings are small implies that wave functions are very small near the rhombus saddle point. We have used the wave functions we computed to determine reduced probability distributions

$$P_r(r_0) = \int_0^\pi d\theta_1 \sin \theta_1 \int_0^\pi d\theta_2 \sin \theta_2 \int_0^{2\pi} d\phi_2 \int_0^\infty dr_1 \int_0^\infty dr_2 \left| \frac{\Psi(\theta_1, \theta_2, \phi_2, r_0, r_1, r_2)}{r_0} \right|^2 \quad (5)$$

$$P_\phi(\phi_2) = \int_0^\pi d\theta_1 \sin \theta_1 \int_0^\pi d\theta_2 \sin \theta_2 \int_0^\infty dr_0 \int_0^\infty dr_1 \int_0^\infty dr_2 |\Psi(\theta_1, \theta_2, \phi_2, r_0, r_1, r_2)|^2 \quad (6)$$

where  $\Psi$  is the wave function obtained from the KEO we used.  $P_r(r_0)$  is defined so that  $\int P_r(r_0) r_0^2 dr_0 = 1$  because it is the amplitude of the wave function that has not been altered by absorbing part of a volume element that is of interest. If  $P_r(r_0)$  or  $P_\phi(\phi_2)$  is large near  $r_0 = 0$  and  $\phi_2 = 0$ , then interconversion is important. For the even  $A$  states, the first state with nonzero amplitude at the saddle point is found at a very high energy (See Figure 3).

## VII. Conclusion

We have used PODVR and spherical harmonic-type basis sets and the Lanczos algorithm to compute vibrational levels of  $\text{Ar}_4$ . We exploit the symmetry of the coordinate symmetry group, a subgroup of the full symmetry group, and use the correlation between it and the full symmetry group to label the levels we compute with irreducible representations of the full symmetry group. This enables us to identify the levels that exist (those whose wave functions are invariant with respect to permutation of the Ar nuclei). Splittings between the even- and odd-parity levels are small, indicating that rearrangement tunneling between the two equilibrium structures is slow. At

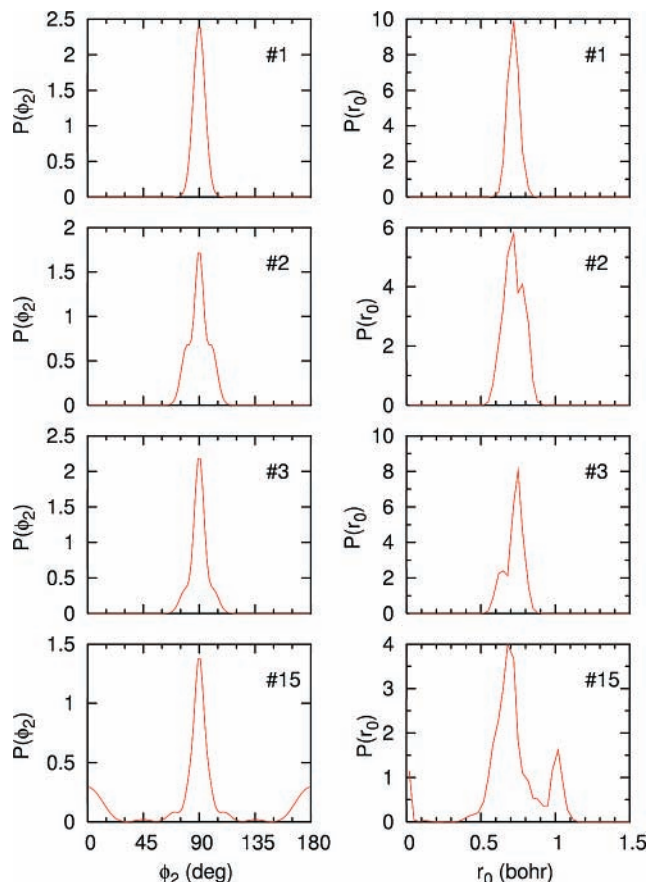


**Figure 3.** Probability distribution functions for  $\phi_2$  and  $r_0$  for selected even-parity bosonic states. State numbers (only counting the bosonic states) are given in each figure. The energies are  $-5.1181$ ,  $-4.8008$ ,  $-4.7250$ , and  $-4.3315$  for states #1, 2, 3, and 15, respectively.

very high energies, some states are found to have appreciable amplitudes near the saddle point.

The CFMC method appears very promising. The main difficulty seems to be the choice of good trial functions. A Monte Carlo method is used to project contributions from higher energy wave functions from the trial functions. If the trial functions are poorly chosen, noise can make it very hard to compute accurate energy levels. In this paper, we point out that using trial functions that depend only on interatomic distances does not enable one to compute odd-parity vibrational states, which exist for any molecule with more than three atoms.

**Acknowledgment.** This work has been supported by the Natural Sciences and Engineering Research Council of Canada. Calculations were done on a computer of the Réseau québécois de calcul de haute performance (RQCHP).

## References and Notes

- (1) Carter, S.; Handy, N. C. *Comput. Phys. Rep.* **1986**, *5*, 115.
- (2) Tennyson, J. *Comput. Phys. Rep.* **1986**, *4*, 1.
- (3) Carrington, T., Jr. *Can. J. Chem.* **2003**, *82*, 900.
- (4) Bramley, M. J.; Carrington, T., Jr. *J. Chem. Phys.* **1993**, *99*, 8519.
- (5) Bowman, J.; Carter, S.; Huang, X. *Int. Rev. Phys. Chem.* **2003**, *22*, 533.
- (6) Carter, S.; Handy, N. C. *Comput. Phys. Rep.* **1986**, *5*, 115.
- (7) Colbert, D. T.; Miller, W. H. *J. Chem. Phys.* **1992**, *96*, 1982.
- (8) Carter, S.; Culik, S. J.; Bowman, J. M. *J. Chem. Phys.* **1997**, *107*, 10458.
- (9) Poirier, B. *J. Theor. Comput. Chem.* **2003**, *2*, 65.
- (10) Dawes, R.; Carrington, T., Jr. *J. Chem. Phys.* **2005**, *122*, 134101.
- (11) Yu, H.-G. *J. Chem. Phys.* **2002**, *117*, 8190.
- (12) Bačić, Z.; Light, J. C. *Annu. Rev. Phys. Chem.* **1989**, *40*, 469.

- (13) Henderson, J. R.; Tennyson, J. *Chem. Phys. Lett.* **1990**, *173*, 133.  
(14) Bramley, M. J.; Carrington, T., Jr. *J. Chem. Phys.* **1994**, *101*, 8494.  
(15) Friesner, R. A.; Bentley, J. A.; Menou, M.; Leforestier, C. *J. Chem. Phys.* **1993**, *99*, 324.  
(16) Luckhaus, D. *J. Chem. Phys.* **2000**, *113*, 1329.  
(17) Bramley, M. J.; Handy, N. C. *J. Chem. Phys.* **1993**, *98*, 1378.  
(18) Bowman, J. M.; Gazdy, B. *J. Chem. Phys.* **1991**, *94*, 454.  
(19) Light, J. C.; Carrington, T., Jr. *Adv. Chem. Phys.* **2000**, *114*, 263.  
(20) Wang, X.-G.; Carrington, T., Jr. *J. Chem. Phys.* **2002**, *117*, 6923.  
(21) Qiu, Y.; Zhang, J. Z. H.; Bačić, Z. *J. Chem. Phys.* **1998**, *108*, 4804.  
(22) Wang, X.-G.; Carrington, T., Jr. *J. Chem. Phys.* **2003**, *119*, 101.  
(23) Wang, X.-G.; Carrington, T., Jr. *J. Chem. Phys.* **2005**, *123*, 154303.  
(24) Wang, X.-G.; Carrington, T., Jr. *J. Chem. Phys.* **2004**, *121*, 2937.  
(25) Yu, H.-G. *J. Chem. Phys.* **2004**, *120*, 2270.  
(26) Yu, H.-G. *J. Chem. Phys.* **2004**, *121*, 6334.  
(27) Ceperley, D. M.; Bernu, B. *J. Chem. Phys.* **1988**, *89*, 6316.  
(28) Bernu, B.; Ceperley, D. M.; Lester, W. A., Jr. *J. Chem. Phys.* **1990**, *93*, 552.  
(29) Cho, H. M.; Singer, S. J. *J. Phys. Chem. A* **2004**, *108*, 8691.  
(30) Nightingale, M. P.; Melik-Alaverdian, V. *Phys. Rev. Lett.* **2001**, *87*, 043401.  
(31) Nightingale, M. P.; Roy, P.-N. *J. Phys. Chem. A* **2006**, *110*, 5391.  
(32) Nightingale, M. P.; Moodley, M. J. *J. Chem. Phys.* **2005**, *123*, 014304.  
(33) Roy, P.-N. *J. Chem. Phys.* **2003**, *119*, 5437.  
(34) Wang, X.-G.; Carrington, T., Jr. *Phys. Rev. Lett.* **2007**, *98*, 119301.  
(35) Blume, D.; Greene, C. H. *J. Chem. Phys.* **2000**, *113*, 4242.  
(36) Brocks, G.; van der Avoird, A.; Sutcliffe, B. T.; Tennyson, J. *Mol. Phys.* **1982**, *50*, 1025.  
(37) Wang, X.-G.; Carrington, T., Jr.; Tang, J.; McKellar, A. R. W. *J. Chem. Phys.* **2005**, *123*, 034301.  
(38) Zare, R. N. *Angular Momentum*; Wiley: New York, 1988.  
(39) This is obtained by using the relation between the spaced-fixed Cartesian coordinates and the vibrational coordinates and Euler angles; see ref 37.  
(40) Wei, H.; Carrington, T., Jr. *J. Chem. Phys.* **1992**, *97*, 3029.  
(41) Echave, J.; Clary, D. C. *Chem. Phys. Lett.* **1992**, *190*, 225.  
(42) Tennyson, J.; Sutcliffe, B. T. *J. Mol. Spectrosc.* **1983**, *101*, 71.  
(43) Bramley, M. J.; Tromp, W.; Carrington, T., Jr.; Corey, G. C. *J. Chem. Phys.* **1994**, *100*, 6175.  
(44) Bunker, P. R.; Jensen, P. *Molecular Symmetry and Spectroscopy*; NRC Research Press: Ottawa, Canada, 1998.  
(45) Dyke, T. R. *J. Chem. Phys.* **1977**, *66*, 492.  
(46) Wang, X.-G.; Carrington, T., Jr. *J. Chem. Phys.* **2003**, *118*, 6946.  
(47) Wang, X.-G.; Carrington, T., Jr. *J. Chem. Phys.* **2001**, *114*, 1473.  
(48) Chen, R.; Guo, H. *J. Chem. Phys.* **2001**, *114*, 1467.  
(49) Henderson, J. R.; Tennyson, J.; Sutcliffe, B. T. *J. Chem. Phys.* **1993**, *98*, 7191.  
(50) Rick, S. W.; Lynch, D. L.; Doll, J. D. *J. Chem. Phys.* **1991**, *95*, 3506.